Solid Earth Discuss., 7, 1–36, 2015
www.solid-earth-discuss.net/7/1/2015/
doi:10.5194/sed-7-1-2015

Solid Earth
Discussions
Open Access

Volcanic soils and landslides: the case study of the Ischia island (southern Italy) and relationship with other Campania events

S. Vingiani[1], G. Mele[2], R. De Mascellis[2], F. Terribile[1], and A. Basile[2]

[1]Department of Agriculture, University of Naples Federico II, Portici (NA), Italy
[2]National Research Council (CNR-ISAFOM), Ercolano (NA), Italy

Received: 27 November 2014 – Accepted: 4 December 2014 – Published: 6 January 2015

Correspondence to: S. Vingiani (simona.vingiani@unina.it)

Published by Copernicus Publications on behalf of the European Geosciences Union.

Abstract

An integrated investigation has been carried out over the soils involved in the landslide phenomena occurred in the 2006 at Mt. Vezzi in the Ischia island (southern Italy). Chemical, physical (i.e. particle size distribution, hydrological analyses and direct measurements of soil porosity), mineralogical and micromorphological properties of three soil profiles selected in two of the main detachment crowns were analysed.

The studied soils, having a volcanic origin, showed a substantial abrupt discontinuity of all the studied properties in correspondence of the 2C horizon, also identified as sliding surface of the landslide phenomena. With respect to the above horizons, the 2C showed (i) as a grey fine ash, almost pumices free, with a silt content increased by the 20 %, (ii) k_s values one order of magnitude lower, (iii) a porosity concentrated in the small size (15 to 30 µm modal class) pores characterized by very low percolation threshold (around 15–25 µm), (iv) occurrence of expandable clay minerals and (v) higher Na content in the exchange complex. Therefore, most of these properties indicated 2C as a lower permeability horizon than the above. Nevertheless, only the identification of a thin (6.5 mm) finely stratified ash layer on the top of 2C enabled to assume this interface as an impeding layer to vertical and horizontal water fluxes, as testified by the hydromorphic features (e.g. Fe/Mn concretions) within and on the top of the layer. Despite the Mt. Vezzi soil environment has many properties (high gradient northern facing slope, similar forestry, volcanic origin of the parent material) in common with those of many Campania debris-mud flows, the results of this study did not support the found relationship between Andosols and debris-mudflows, but emphasize the role of vertical discontinuities as landslide predisposing factor.

1 Introduction

The Italian territory is vulnerable from a hydraulic and geological standpoint, due to its distinguishing geological, geomorphological and climatic factors, along with anthropic pressures. Landslides are frequent and widespread geomorphological phenomena (Guzzetti et al., 1994; Guzzetti and Tonelli, 2004) and the caused damages are severe. In the last 60 years (1960–2012), all the 20 Italian regions have suffered fatal events – ANSA (2013) census with data from CNR-IRPI: 541 floods in 388 municipalities caused 1760 casualties (762 killed, 67 missing, 931 injured) and 812 landslides in 536 towns produced 5368 casualties, for a total of 3413 deaths, including the tragic event occurred in Vajont on 1963 (1917 killed, 14 missing, 1941 wounded) (Ward and Day, 2011). The Campania is the third region in Italy for number of landslide events (363). In the ecosystems of this Region, the most dangerous type of landslide are debris and mudflows, i.e. very rapid to extremely rapid flows of detritic and plastic materials having high water content (Hungr et al., 2001). One of the most catastrophic historical event occurred at Sarno on 4 and 5 May 1998: debris and mudflows, detached from the slopes of Pizzo D'Alvano, extended 3–4 km into the surrounding lowlands, causing the lost of 161 human lives and severe destruction. Anyhow, other disastrous events struck the mountainous reliefs of the Region before and after the events of Sarno. Soil properties and relationships between debris-mudflows and soil type were investigated on twenty catastrophic landslides occurred in Campania (Terribile et al., 2000, 2007). The results showed that the most catastrophic events are related to soils developing upon pyroclastic materials, covering the carbonatic relieves of the Campania Apennines, and belonging to the Andosols group, generally Molli-Vitric e Pachi-Vitric Andosols (WRB, 2014). In these soils the aspect of the slope affects soil susceptibility to landslide triggering and the landslide susceptibility is related to the hydrological properties, which induce higher water storage especially in northern facing soils. In another study on the soils related to the Sarno landslide it was found (Basile et al., 2003) an increase in soil water storage, due to anisotropy of vertical hydraulic conductivity and water retention

characteristics, connected to the occurrence of soil discontinuities (e. g. soil mantle cutting due to track ways) and it was demonstrated that landslide susceptibility is also strongly affected by human-induced disturbances to forestry ecosystems.

Therefore, when five debris-mudflows were triggered on 30 April 2006 on the northern slope of Mt. Vezzi in the Ischia Island and caused 4 victims, an investigation aimed to assess the occurrence of andic properties also in the Ischia soils was carried out, due to the close similarity of the environments (volcanic), type of landslides (debris-mudflows) and aspect of the slope (northern) with those of the other Campania landslides.

Hence, the principal aim of this work was to investigate the soil properties (chemical, physical, hydrological, mineralogical and micromorphological) at Mt. Vezzi, in order to (i) define whether soil properties may have a role in determining these landslides, (ii) verify if the relationship between Andosols and debris-mudflows, as occurred for most catastrophic Campanian landslides, is still valid for the Ischia landslides and (iii) carry out a detailed investigation at microscale of the sliding surface in order to understand causes of the occurred events.

1.1 Events and geomorphological data related to landslides area

Five landslides (namely f1 to f5, following Ascione et al., 2007) (Fig. 1b) occurred on 30 April 2006 along the northern slope of Mt. Vezzi, in two times. The eastern three landslides (f1 to f3) occurred firstly (around 7 a.m.), while the western ones (f4 and f5) about one hour later. The source area is located in the uppermost Costa Ruscello hillslope, in a narrow belt (between 315 and 345 m a.s.l.) close to Mt. Vezzi summit, characterised by high slope gradient (35–45°) and variable morphology: f1 initiated at the outer rim of an access track, f2 to f5 started very close to the Costa Ruscello summit free face (Ascione et al., 2007; De Vita et al., 2007). The landslides were classified (De Vita et al., 2007) complex debris slide – debris flows (Cruden and Varnes, 1996). Data recorded before the events, on 29 and 30 April, by the closest meteorological station (Forio d'Ischia, approximately 6 km far from Mt. Vezzi, at 150 m a.s.l., rain gauge

records reported by Mazzarella and De Luise, 2009) evidenced that rainfall was barely 14 mm. Nevertheless, reliable witnesses reported that landslides were preceded by 12 h of intense rainfall.

1.2 Geological and environmental setting

The Ischia island represents the emerged part of a large active volcanic complex rising more than 1000 m a.s.l., located in the easternmost portion of the Naples city area (Fig. 1c); together with the Procida island and the Campi Flegrei caldera, it constitutes the Phlegrean volcanic district (De Vita et al., 2010). Mt. Vezzi (392 m a.s.l.) is located in the south-eastern area of the island and, together with Mt. Torrione (375 m a.s.l.), belongs to a group of relics of a major volcanic complex related to a phase of the island volcanism (Rittmann and Gottini, 1980; Vezzoli, 1988; Civetta et al., 1991). The top of Mt. Vezzi consists of a lava dome (Di Nocera et al., 2007) covered by the Piano Liguori Formation, pyroclastic products of the recent hydromagmatic explosive activity (about 5347–5807 years BP, ^{14}C calibrated) (Orsi et al., 1996), made up by trachytic ash and pumice layers. Different land use characterises the summit landscape and the north slope, with vineyards occurring on Piano Liguori and close surrounding slopes, and chestnut coppice woodland on high gradient northern slopes. The woodland appears poorly managed in the areas of the detachment crowns, because of clear signs of unplanned cuttings and evidences of anthropic disturbances, like dense trail network and fire traces on tree barks.

2 Materials and methods

The first survey on the detachment crowns of Ischia landslides was done in the period just after the events (on 12 May 2006) and first soil samples analysed (Vingiani and Terribile, 2007). Nevertheless the pedological study and the sampling was carried out only during the following summer, due to the wet state of the deep soil horizons limiting

the digging. Two (f2 and f3) of the five detachment crowns were studied (Fig. 1a): P1 and P2 profiles were described and sampled in f2 and P3 in f3, following the guidelines of FAO (2006). Bulk and undisturbed soil samples were collected for chemical, physical (particle size distribution and hydraulic properties) and microtomographic analyses. For soil classification, the WRB system was used (WRB, 2014). Two field sensitivity tests were used in order to estimate the soil andic properties: (1) one test enables to evaluate the thixotropy (smeary upon pressure) on moist undisturbed soil samples applying a simple pressure between fingers (Wells and Furkert, 1972), because if allophanes (therefore andic properties) occur in soils, the material become sensitive and suddenly shears under increasing pressure; (2) the other test evaluates the amount of non-crystalline (amorphous) material in soil: the action of the sodium fluoride (NaF) upon non-crystalline soil material induces release of hydroxide ions (OH^-) to the soil solution and increases the pH (Fields and Perrott, 1966).

2.1 Chemical analysis

Soil bulk samples were air dried and sieved at 2 mm. Percentages of coarse fragments ($\varphi > 2$ mm) and fine earth fraction ($\varphi < 2$ mm) were measured after sieving. Chemical analysis were carried out on the fine earth fraction, according to the Soil Survey Laboratory Methods Manual (USDA, 2004): the soil pH was determined potenziometrically on soil–H_2O (1 : 2.5 ratio) and soil–solution (KCl 1M and NaF 1M, 1 : 2.5 and 1 : 5 ratios, respectively) suspensions; the organic carbon (OC) content following the Walkley and Black (1934) procedure; the cation exchange capacity (CEC) according to Mehlich (1938), with barium chloride-triethanolamine buffered at pH 8.2, and the exchangeable cations (Ca, Mg, Na, K) were measured by ICP-AES Varian Liberty model 150; the phosphate retention according to Blakemore et al. (1987); the electrical conductivity (EC) was measured on soil–H_2O (1 : 5 ratio) suspensions. The sodium adsorption ratio (SAR) was calculated (Lesch and Suarez, 2009) as the square root of the ratio of the measured exchangeable sodium (Na) to calcium + magnesium (Ca + Mg), divided for

two, while the exchangeable sodium percentage (ESP) was calculated as the percentage ratio of the Na to the CEC.

Due to the volcanic origin of the parent material, specific analyses were also required in order to assess occurrence of andic properties. Selective extraction procedures were applied to soil samples and the different Al, Fe and Si forms were determined. The acid ammonium-oxalate extractable forms (Al_o, Fe_o and Si_o) were obtained after Schwertmann (1964) and Blakemore et al. (1987), the Na-dithionite citrate bicarbonate (DCB) extractable components (Al_d, Fe_d and Si_d), also called total "free iron oxides", by the Mehra and Jackson (1960) procedure and the Na-pyrophosphate extractable complexes (Al_p and Fe_p) according to Bascomb (1968). The concentration of elements was then measured by ICP-AES Varian Liberty model 150. Allophane and ferrihydrite contents were calculated using Parfitt (Parfitt and Wilson, 1985; Parfitt, 1990) and Childs (1985) formulas, respectively.

2.2 Hydrological analysis

Hydrological analyses were carried out on undisturbed soil samples (φ = 86 mm, h = 150 mm) collected in selected horizons of the P2 (Bw_1, Bw_2, Bw_4, 2CB, 2C) and P3 (Bw_4, 2C, 2Btb) profiles. The saturated hydraulic conductivity, k_s, was measured by means of a constant head permeameter (Reynolds and Elrick, 2003). The soil water retention, $\theta(h)$, which is the relationship between water content θ and water pressure head h, and the hydraulic conductivity, $k(\theta)$, which is the relationship between hydraulic conductivity k and water content θ, were both determined applying the evaporation method (Arya, 2002). The undisturbed soil samples were slowly saturated from the bottom. Three tensiometers were installed at three different depths in the samples and placed on a load cell; starting from saturation and during a 1-dimensional transient upward flow, pressure head and weight of the sample were automatically recorded at these depths until air was observed in the circuit of the uppermost tensiometer. After that, the soil sample was dismantled and placed for 24 h in the oven at 105 °C to determine the water content from the weight data set. An iterative method was applied to

obtain the $\theta(h)$ relationship (Basile et al., 2012). The unsaturated hydraulic conductivity curve was obtained applying the method proposed by Watson (1966). Details on the calculus procedure can be found in Bonfante et al. (2010).

2.3 Physical and microtomographic analyses

The particle size distribution (PSD) was determined on soil samples after dispersion with Na-hexametaphosphate and the measurements were carried out by the laser diffraction technique, using a Malvern Mastersizer 2000 system (Glendon and Dani, 2002).

X-ray micro-tomography was performed in order to reconstruct 3-D images of the inner structure of the soil samples collected from three subsurface contiguous horizons identified in the P2 profile. The SKYSCAN 1172 desktop system (www.skyscan.be), based on a microfocus cone beam X-ray source, was used and an optimised inverse Radon transform (Kak and Slaney, 1988) was applied on the X-ray attenuation coefficient dataset for image reconstruction. Then the "successive opening" image analysis algorithm (e.g. Serra, 1982; Horgan, 1998) was applied on the reconstructed 3-D images in order to obtain a Pore Size Distribution (PoSD) consisting in the pore space classification according to the wall spacing. Finally the procedure of Lantuejoul and Maisonneuve (1984) was applied to calculate the percolation curves in order to evaluate the connectivity of the pore space.

The inter-aggregate PoSD of each horizon was calculated scanning undisturbed soil samples collected with cylinders in PMMA 3.4 cm in height and diameter, then a 3.5 cm^3 cubic Region Of Interest (ROI) was reconstructed at 30 µm pixel size (image resolution). The intra-aggregate 3-D pore structure was reconstructed and analysed on a 3.5 mm^3 ROI at 1.5 µm image resolution scanning on two selected aggregates from the bulk samples, separately.

In addition, a pore size distribution was derived from the hydrological analysis. Specifically, the scale of the soil water pressure head on the axis of the soil water retention curve can be replaced by that of the diameter of the capillaries according to

the capillarity law $|h| = 2\sigma\cos\gamma/r\rho_w g \approx 0.3/d$ for length units in cm. This procedure supplies the cumulative pore size distribution curve. The derivative of this curve is the curve of pore size density distribution. Such a schematization, which assumes the simple conceptual model of the soil porous system as a bundle of parallel capillaries to be correct, leads to the derivation of the "equivalent" pore size distribution. In this manner the equivalent diameters are those of the bundle of capillary tubes, which behave, in functional terms, as the soil sample.

2.4 Mineralogical and micromorphological analyses

Mineralogical analyses were carried out by means of X-ray diffractometry (XRD) on sand, silt and clay fractions. Samples were dispersed by the use of Na-hexametaphosphate and separated in different sizes by means of sieving, for sand fraction, and centrifuge, for clay fractions. The clay fraction was saturated using $CaCl_2$ and washed with water and ethanol, till removal of chlorides. Mineralogical spectra were acquired with a Rigaku Geigerflex D/Max IIIC, CuKa radiation, Ni filtered, at 35 kW and 35 mA. Powder samples of sand (2 mm–50 µm), silt (50–2 µm) and clay (< 2 µm) fractions were analyzed randomly, in order to detect primary and secondary minerals.

Undisturbed samples collected by means of Kubiena boxes for micromorphological studies were impregnated with crystic resin and large (15 × 7.5 cm) thin sections were produced using the FitzPatrick methodology (1984, 1993). The micromorphological description referred to the terminology used by FitzPatrick (1993).

3 Results

3.1 Soil morphology and main chemical properties

All the studied soils (Table 1) were very deep, characterised by thin (about 5 cm) brownish surface horizons (A), covering dark yellowish brown Bw horizons abruptly overlying

greysh brown to light brownish grey 2C horizons, at a variable depth from 70/90 to 190 cm. The yellowish and greyish colours suggested a generally low degree of weathering of the soil and ashy materials, as a consequence of scarce iron oxides formation. Both tests for field identification of andic properties resulted negative, showing absence of thixotropy and andic properties. All horizons did not reacted to 10 % hydrochloric acid (HCl) due to the absence of carbonates. The soil structure of all soils abruptly changed from sub-angular blocky of the Bw horizons to massive of the ashy layer of the 2C horizons. During the sampling, the soil horizons showed also very different moisture status: the A and all the Bw horizons were slightly moist, while the massive 2C was wet and limited the digging to 100 cm of depth, just after the landslide events. Moreover, the authors of the survey referred that "jumping on the 2C appeared similar to jump on a waterbed", a kind of "blob effect" which indicated a high plasticity of the wet 2C horizon. Therefore, in order to collect undisturbed samples of the 2C and underneath horizons, it was necessary to postpone the sampling in dryer soil conditions. Anyhow, the above described 2C horizon was found in all the studied soil profiles and identified as sliding surface of the occurred landslides (De Vita et al., 2007). In P1 and P3, a yellowish-red 2Btb horizon of a buried soil, having a moderate sub-angular blocky structure, was found below the 2C. Very few to few roots occurred in A and Bw horizons, but they were always absent in 2C and 2Btb.

The results of the chemical analyses showed large accumulation of organic carbon (46.1–71.3 $g\,kg^{-1}$) (Table 2) in all A horizons. As expected, the OC rapidly decreased with depth (Bw_1 horizons: 12.3–6.0 $g\,kg^{-1}$; 2C horizons: 0.8–1.2 $g\,kg^{-1}$). A similar trend was followed by the CEC, whose highest values – as expected – were found in correspondence of the A horizons. Soils had a generally neutral reaction (pH_{H_2O}) and the pH was weakly increasing in correspondence of the 2C horizons (Table 2). The soil pH measured in KCl solution (pH_{KCl}) was lower of 1 to 2.5 units than pH_{H_2O}, which suggested a potential exchangeable acidity (due to H^+ and Al^{3+} ions) particularly high for the 2C horizons (values between 2.0 and 2.5). Despite the exchangeable complex was dominated by the Ca, high Na + Mg contents (40–65 %) were measured in the

deepest horizons of the three profiles, which showed also a calculated exchangeable sodium percentage (ESP) generally higher than 15 %. Nevertheless, they cannot be classified as salic or natric horizons (WRB, 2014), for lack of requirements in terms of electrical conductivity (EC < 15 dS m^{-1}), soil structure and texture. Data from the selectively dissolved procedures showed for all the soils generally low values of % $Al_o + 0.5Fe_o$ (AI = andicity index), ranging from 0.1 to 0.7, as well as low allophane (0.9–2.6 %) and ferrihydrite (0.1–0.6 %) contents (Table 4). The low AI, associated with the low phosphate retention – Pret – (2–35 %) (Table 4), evidenced that generally these soils did not satisfy the requirements for Andosols classification (WRB, 2014), except for the P1, which falls in the Andosols just at the limit with the Cambisols. Therefore they were classified: P1 – Vitric Andosol (loamic, novic, sodic), P2 – Sodic Cambisol (loamic, tephric) and P3 – Sodic Cambisol (loamic, colluvic, novic, tephric). Moreover, the Na-pyrophosphate extractable forms (Al and Fe-humus complexes) were always absent, according with the very low Al_p/Al_o ratios (< 0.4), even in the most rich of OC (71.3 g kg^{-1}) horizon. The calculated Fe_o/Fe_d ratios showed values generally decreasing with depth (from 0.7 to 0.1), which enabled to suppose a higher degree of weathering of the deeper horizons compared with the upper.

3.2 Physical properties

3.2.1 Particle size distribution (PSD)

The rock fragment ($\varphi > 2$ mm) distribution showed the highest pumices content in A and B horizons (Table 3). The medium size (5–20 mm) pumices ranged from few (3–4 %) to many (18–22 %) in A and B horizons, while only few (around 1 % or less) and very fine (2–5 mm) pumices were found in all 2C horizons and in 2Btb of both P1 and P3 (data not shown). Concerning the fine earth fraction, the A and most of Bw horizons were sandy loam, even the former resulted coarser compared with the latter, while few Bw, the 2BC, 2CB and 2C were silty loam (Table 3), due to the higher silt content (more than 50 %). By the analyses of the particle size distribution curves, all

the horizons showed a bimodal PSD. Generally, A and Bw horizons (Fig. 2a and c) exhibited a stronger bimodal distribution of soil particles, one population having a peak at a diameter around 30–50 µm and another of 600–900 µm. Very different revealed the PSD of the 2C horizons (Fig. 2b and d), having a much less pronounced or as a whole a unimodal distribution, in which the most abundant population had a diameter around 30 µm. The PSD of the Bw_4 showed intermediate characters between the Bw series and the underlying 2C horizons. Therefore, the above data are consistent with the discontinuity (found in field) in terms of morphological and chemical properties.

3.2.2 Hydraulic properties

All the investigated horizons showed high water retention capacity. Values of saturated soil water content ranged from 0.56 to 0.64 cm^3 cm^{-3}, with a slight decrease from the surface to the bottom of the soil profile. Despite the soils did not exhibit andic properties, these high values were indicative of a complex porous system, similar to that shown by Andosols, which are well known for their high water retention capacity (Basile et al., 2007). The water retention curves and the equivalent pore size distributions of selected horizons of P2 were reported in Fig. 3a and b, correspondingly. The water retention curves of the Bw horizons showed a smoothed shape underlying a rather platicurtic equivalent pore size distribution, indicating the presence of a wide range of pore diameters (Fig. 3b). Moreover, the Bw water retention curves exhibited a slight bimodality, with a secondary porous system having an equivalent pore dimension ranging between 1 and 10 mm. This behaviour is common in many natural soils in which the presence of aggregates frequently results in a water retention curve having at least two points of inflection (Coppola, 2000). Different was the shape of the 2C retention curve, which almost overlapped to the others till around 20 cm, but sharply decreased between 100 and 1000 cm. This trend is related to a leptokurtic distribution of pore size (Fig. 3b), with the prevailing class at 10 µm. An intermediate trend between the Bw horizons and the 2C was shown by the retention curve of the 2CB.

The unsaturated hydraulic conductivity curves of selected horizons of P2 were shown in Fig. 3c. In the range of pressure head where the measured curves overlap (h between −190 and −330 cm), the 2C horizon showed higher unsaturated hydraulic conductivity with respect to the upper horizons. This is consistent with the higher slope showed by the 2C water retention curve in the same explored range. In fact, the relative hydraulic conductivity at a specific value of pressure head is function of the slope of the water retention curve in the same point, more than its absolute value (Basile et al., 2006; Kutilek and Nielsen, 1994). Moreover, the values of the saturated hydraulic conductivity decreased with depth (Table 3). Indeed, the highest values were found in correspondence of the upper Bw horizons ($k > 100\,\mathrm{cm\,h^{-1}}$), while they decreased one order of magnitude for Bw_4 and 2CB in P2 (k = 80.7 and 23.3 $\mathrm{cm\,h^{-1}}$) and two order of magnitude for 2C in P2 ($k = 5.5\,\mathrm{cm\,h^{-1}}$), while in P3 the decrease was of one order of magnitude between Bw_4 and 2C. The different rank along the depth of the saturated and unsaturated hydraulic conductivity is not surprising because they apply to different pore ranges.

3.3 Optical microscopy

A selection of results of the micromorphological analyses of P2 were reported in Fig. 4. The surface A horizon showed a very fine granular structure, presence of living roots and blackish granules of decomposed organic residues (Fig. 4a), typical characters of forestry soils. The following Bw horizon, characterised by a granular structure, exhibited very abundant (from 25 to 50 %) and generally no weathered pumice fragments, enveloped by silty – fine sandy brown material (Fig. 4b). A clear microstructure change was observed in correspondence of the deeper 2CB horizon, characterised by an incomplete sub-angular blocky structure less porous than the above. Chaotically immersed in the soil matrix, angular to sub-angular peds (Fig. 4c_1 and c_2) pseudo-stratified with finer brownish and coarser materials were found and interpreted as fragments of the underlying horizon (2C), probably originated by the pedofauna activity. The soil matrix and some aggregates of 2CB showed clay coatings occurrence in pores and

likely neogenetic clays in pumice fragments (Fig. 4d_1 and d_2), both indicating weathering processes in place.

The following 2C horizon showed a thin stratification in the upper 6–7 mm, which was commonly incrusted by Fe-Mn segregations (Fig. 4e). Moreover, in a root pore localised just above the described stratification and having its same direction, anisotropic clay films and frequent Fe-Mn segregations (Fig. 4g_1 and g_2) coated the walls. The combination of these features are likely accountable of the massive silty ash layer described in field (Table 1) and identify a low drainage soil environment, favouring waterlogging and hydromorphic conditions (possibly temporary). In the lower part, the 2C horizon became coarser due to the occurrence of a layer having a mineral single grain structure, with pores filled by clay materials (Fig. 4f_1 and f_2).

3.4 Microtomographic analyses

Hydrological data provided an indirect evaluation of the pore organisation through the equivalent pore size distribution; however a direct evaluation of the real pore size distribution was achieved by the image analysis. The inter-aggregate and the intra-aggregate porosity were investigated using different image resolution limits, 30 and 1.5 µm, respectively (pores smaller than pixel resolution cannot be detected). These values roughly correspond to −100 and −2000 cm of pressure head, according to the capillary law. In Fig. 5b-1 the inter-aggregate PoSD (> 30 µm) of three significant P2 soil horizons (Bw_4, 2CB, 2C) was reported. The three curves exhibited a very similar shape, asymmetric unimodal to the right. The Bw_4 was characterised by the highest porosity (36.2 %), which was calculated by integrating the area under the curve, by the highest modal value (210 µm) of pore size and the widest range of pore size variability, with the largest pores reaching a size of 2 mm; on the contrary, the 2C had the lowest porosity (only 6.7 %), the lowest modal value of pore size (150 µm) and the largest pore size reached 1 mm, even if the pore sizes most frequently found were below 550 µm (Fig. 5b-1). Measurements of inter-aggregate connected porosity were reported vs. increasing "occluded" pore size, in the three spatial directions by the percolation curves

(Fig. 5b-2). They represent the percentage of pore volume which connects opposite faces of the ROI after virtual occlusion of pores of increasing size. The curves of the 3 selected soil horizons exhibited different values of initial (no pore occlusion) connectivity and percolation thresholds (pt). The pt represented the maximum diameter which guarantees the connectivity in a defined space direction. Therefore, the percolation curves allowed to identify also critical sizes of pores limiting fluid and solute transport in any direction. All samples showed an isotropic initial connectivity with the highest and lowest value for Bw_4 and 2C, respectively. Results on the z axis (Fig. 5b-2) showed a pt occurring in correspondence of Bw_4 for higher (510 µm) values of pore size, compared with 2C (330 µm) and 2CB (270 µm). Since the 2C connected porosity was only 11 % at 270 µm, data of 2C and 2CB can be considered very similar. Not very different revealed the pore connectivity along the other two (x, y) directions (the horizontal plane), where the 2C horizon showed the lowest pt at 210 and 150 µm in x and y axis, respectively. Therefore, in the range of the detected pore size (> 30 µm), data seem to suggest occurrence in the soil profile of an isotropic highly permeable horizon (Bw) overlaying horizons with lower permeability (2CB and 2C). By the comparison of the porosity assessed by means of hydrological measurements and that obtained by inter-aggregate microtomographic analyses (pores larger than 30 µm), as expected the first data resulted higher for all the analysed horizons, with the largest difference found for the 2C (Table 5). The discrepancy of data is mainly due to the resolution applied and the largest difference was found for the 2CB and 2C horizons, because they were formed mainly by pore smaller than 30 µm. Therefore, in order to better investigate the porosity of the 2C horizon, due to its important role as sliding surface, data of intra-aggregate porosity were successively acquired on 2C using a resolution limit of 1.5 µm (Fig. 5c-1). Results showed the occurrence of two main types of aggregates building this horizon: aggregate type I, with internal massive microstructure and aggregate type II, having a micro fibric structure; both were characterised by high porosity (43.9 and 60.7 %, respectively) made by small pores (15 and 30 µm modal class, respectively) (Fig. 5c-1). By the analysis of the pore connectivity (Fig. 5c-2), the 100 % of pores was

interconnected in each direction but the percolation thresholds were very low (around 15–25 µm). The latter result, combined with the very high porosity values of small size, fully agree with the high water retention found by the hydrological analyses in correspondence of such horizon. In fact the full connectivity of the intra-aggregate pore network allows the complete water saturation of the 2C horizon, while the small size pores with low percolation thresholds require high energy to remove water from such a pore system.

3.5 Clay mineralogy

As a whole, K-feldspars (peaks at 0.647, 0.334, 0.324 and 0.321 nm) and mica (0.994, 0.448, 0.332, 0.257 nm) were the minerals found in the sandy and silty fractions of both soil horizons and ash deposits (2C horizons) (data not shown), consistently with the mineralogy of the Phlegrean rocks (Di Vito et al., 2008). On the contrary, the XRD patterns of the clay fraction (Fig. 6) showed differences between the A-Bw horizons vs. 2CB-2C. Indeed, all horizons exhibited kaolinite (0.711, 0.445, 0.356 nm), mica-illite (0.998, 0.495 nm), K-feldspar (0.333 nm) and analcime (0.555 nm) peaks occurrence, while only 2CB and 2C showed ∼ 1.4 nm peaks (1.48 nm) in the Ca saturated samples. After EG treatment, the ∼ 1.4 nm peaks shifted to ∼ 1.6 nm (Fig. 6), due to the expandable nature of these clay minerals, and they were identified as smectites.

4 Discussion

4.1 The Ischia soil properties

As a whole, the results of the pedological study carried out on some detachment crowns of the Mt. Vezzi landslides show the occurrence of soils ranging from weakly to moderately developed in terms of soil structure, organic matter accumulation in the subsurface horizons, degree of weathering of the rock fragments and iron oxides formation. Despite these soils originate by volcanic parent material, they do not exhibit andic

properties (WRB, 2014) but only incipient vitric properties in few horizons of the P1. As well as other volcanic soils, the Ischia soils exhibit both large – spatial (horizontal) and vertical variability between pedons, in terms of chemical and physical properties. The main abrupt variation of soil properties is identified at variable depth between 70/90 and 190 cm, where pumice bearing soil horizons (A and Bw) overly fine ashes (2CB and/or 2C) with a silt content increased by the 20 %. Accordingly, also the physical, micromorphological and mineralogical properties change. Indeed, the inter-aggregate porosity, investigated by means of the microtomographic analyses, shows significant differences between the Bw and 2C horizons in terms of: (i) total porosity larger than 30 µm (36.2 and 6.7 %, respectively), (ii) mode of pore size distribution (210 and 150 µm, respectively), (iii) pore size, which is larger in Bw (till 2 mm) than in 2C (till 1 mm) and (iv) connected porosity (percolation threshold at around 500 µm and 150–225 µm pore size, respectively). Moreover, the intra-aggregate (in the range 30–1.5 µm) connected porosity, measured only in the 2C, shows the occurrence of aggregates characterised by high total porosity (from 60.7 to 43.9 %) made by small pores (15 to 30 µm modal class) and very low percolation threshold (around 15–25 µm), which cause a lower permeability of the pore network. These data are consistent with the general decrease of saturated hydraulic conductivity (k_s) also observed with depth, where the lowest values are found in correspondence of 2C. Nevertheless, the k_s value of 2C is still high and the authors believe that this horizon cannot be considered an impeding layer (i.e. horizon having a low k_s value) or a waterlogging plane. By the comparison of the k_s by the laboratory (in this paper) and those by the field (De Vita et al., 2007) on the same soil horizons (the Bw are named B, the 2CB is C_1 and the 2C is C_2 in De Vita et al., 2007), it was observed: (i) generally lower values of k_s measured in field (1×10^{-2} cm s^{-1} measured for B and 1×10^{-5} cm s^{-1} for 2C) than those measured in laboratory (see Table 3), but (ii) consistent trends between laboratory and field data, both characterised by decreasing values with depth. Despite the field measurements of k_s by the literature are lower than those obtained by the laboratory, due to the different methodologies applied and the experimental procedures carried out in different environmental conditions (Basile

et al., 2007), the field data of 2C are two orders of magnitude lower than the laboratory (10^{-5} and 10^{-3} cm s^{-1}, for the first and latter data, respectively). Therefore, if we only look at the field data, the very low values of k_s really indicate 2C as impeding layer, but this is in opposition to what reported above by the evaluation of the laboratory k_s measurements. The results of the micromorphological analyses enabled to clarify this incongruity. Indeed, the occurrence of the thin (6.5 mm) slightly porous layer, made by finely stratified ashes, at the interface 2CB/2C in P2, very likely represents an obstacle to vertical and horizontal water fluxes, as testified by the hydromorphic features (e.g. Fe/Mn concretions) found on the top and within the layer. The 2CB is interpreted as the upper part of 2C reworked by the pedofauna activity. Due to the very low thickness, the authors suppose that the stratified layer was not sampled for the hydrological laboratory measurements, therefore it did not affect the results.

The presence of clay coatings in the pore space of 2CB and 2C very likely increased the conditions of waterlogging created by the thin ash layer above 2C, because the swelling clay particles, expanding during hydration, also reduce the pore space for water fluxes. This process is certainly increased by the occurrence of Na, which has been found in the soil exchange complex of the deepest horizons, because this cation causes clay hydration and deflocculation, which deteriorate the soil physical properties (Basile et al., 2012). The origin of the Na in these soils is likely related to the alkaline trachytic composition of the volcanic ash.

4.2 Comparison between the Ischia and the other Campania soils affected by debris-mudflows

Despite the common landform (northern facing slope with high gradient), the similar forestry (mixed chestnut woodland – coppice), the volcanic origin of the parent material, the same movement type of the triggered landslides, the results of this study evidence significant differences in terms of peculiar properties between the Mt. Vezzi (MV) and the other Campania (CA) soils involved in debris-mudflows. Indeed, as a whole, both MV and CA are characterized by shallow surface horizons, which store the most

OC content of these soils (49–71 and 28–98 g kg^{-1}, respectively), and thick deep horizons, which generally show lower OC content in MV than in CA (2.3–12.3 and 2.2–32.7 g kg^{-1}, respectively). Similar soil reaction (pH ranging between 6.0 and 7.6 in MV and 6.5–8.3 in CA) and comparable saturated water content (0.44–0.64 and 0.50–0.75 cm^3 cm^{-3}, MV and CA, respectively) are found in both soils, along with saturated hydraulic conductivity, which is generally high and decreasing with depth. The difference between MV and CA occurs essentially in terms of andic properties: the former soils do not exhibit andic properties, while the latter are well developed Andosols. As a consequence, also the thixotropy is absent in MV while is well development in CA, consistently with the degree of development of the andic properties. The difference in andic properties is probably due to the climatic conditions of the pedogenetic environments, which strongly affect the andosolization processes (Shoji et al., 1993). In particular, the average of the yearly rainfall between the 1960 and 1990 years (data from ISPRA – SINTAI, 2005) shows that Ischia (Ischia Ponte – Pilastri station registered an average annual rainfall of 850 mm) is dryer compared with the inland areas of the Campania Region (Montevergine station registered an average annual rainfall of 1857 mm).

Therefore, the occurrence of debris and mud-flows in "non-andic" soils, like those of MV, enables to give more and stronger relevance, in terms of predisposing factor to landslides occurrence, to the abrupt even microscopic spatial variability of the soil (physical) properties.

5 Conclusions

The results of the study carried out on Mt. Vezzi enabled to identify generally young and deep volcanic soils showing incipient vitric properties but not andic properties. Therefore, within the landslide phenomena occurred in the Campania Region, the soil properties at Mt. Vezzi do not confirm the relationship between debris/mud-flows and Andosols previously found for the Campania Region (Terribile et al., 2007). In this respect the climatic conditions seem to play a key role in the differentiation of soils. Nevertheless, the Mt. Vezzi and the other CA sites have in common the significant vertical variability of soil properties, besides environmental factors. Specifically, at Mt. Vezzi a significant discontinuity was identified at variable depths (70/90–190 cm) at the interface B–2C horizons, in terms of physical (i.e. different particle size distribution, pore size and connected porosity, anisotropy of hydraulic conductivity), chemical (i.e. Na enriched deep horizon) and mineralogical (i.e. swelling clays only in the deep horizons) properties. Moreover, the identification of the thin finely stratified ashy layer above 2C, by means of the optical microscopy, emphasized the role of the 2C as sliding surface. Indeed, this layer further reduces vertical and horizontal water fluxes and lead to the increase of soil water storage in the overlying soil, when heavy rainfall events occur and produce an increased instability of the slope because of the greater soil weight.

As resulting by the observations on Mt. Vezzi landscape and on the other CA, these are very fragile ecosystems due to the frequent human-induced disturbances, consisting of soil mantle cutting due to track ways and unplanned cuttings of woodlands, which could increase the water stored in the profile from about 30 to 45 % (Basile et al., 2003). Therefore, with the aim to safeguard these precious (for example in terms of biomass production) and highly vulnerable forest ecosystems, it is emphasized the must for further investigations on the spatial distribution of both (i) high soil thickness above "impeding layers" and (ii) road cut/natural steep walls, in order to identify the "highest risk areas" to landslides.

Author contributions. S. Vingiani, R. De Mascellis and F. Terribile sampled the soils in the landslide detachment crowns. S. Vingiani designed the experiments and carried out the chemical and the mineralogical analyses. S. Vingiani and F. Terribile analysed soil thin sections by means of the micromorphological methodologies. A. Basile and R. De Mascellis designed and performed the physical measurements. G. Mele planned and carried out the microtomographic analyses. S. Vingiani and A. Basile prepared the manuscript with contributions from all co-authors.

Acknowledgements. The authors thank Luciana Minieri (Department of Agriculture – University of Naples Federico II) and Nadia Orefice (CNR ISAFOM – Ercolano NA) for the measurement of some chemical and physical soil properties.

References

ANSA: Vittime delle alluvioni (1960–2012), available at: http://ansa.it/web/notizie/photostory/primopiano/2013/11/19/Vittime-alluvioni-1960-2012-_9646757.html?idPhoto=1, 2013.

Arya, L. M.: Wind and hot-air methods, in: Methods of Soil Analysis. Part 4. Physical Methods, SSSA Book Series 5, SSSA, Madison, 916–926, 2002.

Ascione, A., Cinque, A., Franza, A., and Romano, P.: The geomorphic control on the initiation and propagation of the Mt. Vezzi landslides (Ischia island, Italy) occurred on 30th April 2006, Italian Journal of Engineering Geology and Environment, 2, 93–118, 2007.

Bascomb, C. L.: Distribution of pyrophosphate extractable iron and organic carbons in soils of various groups, J. Soil Sci., 19, 251–268, 1968.

Basile, A., Mele, G., and Terribile, F.: Soil hydraulic behaviour of a selected benchmark soil involved in the landslide of Sarno 1998, Geoderma, 117, 331–346, 2003.

Basile, A., Coppola, A., De Mascellis, R., and Randazzo, L.: Scaling approach to deduce field unsaturated hydraulic properties and behavior from laboratory measurements on small cores, Vadose Zone J., 5, 1005–1016, 2006.

Basile, A., Coppola, A., De Mascellis, R., Mele, G., and Terribile, F.: A comparative analysis of the pore system in volcanic soils by means of water-retention measurements and image analysis, in: Soils of Volcanic Regions in Europe, Springer, Berlin, 493–513, 2007

Basile, A., Buttafuoco, G., Mele, G., and Tedeschi, A.: Complementary techniques to assess physical properties of a fine soil irrigated with saline water, Environ. Earth Sci., 66, 1797–1807, 2012.

Blakemore, L. C., Searle, P. L., and Daly, B. K.: Methods for Chemical Analysis of Soils, N.Z. Soil Bureau Sci. Rep. 80, Soil Bureau, Lower Hutt, New Zealand, 1987.

Bonfante, A., Basile, A., Acutis, M., Perego, A., and Terribile, F.: SWAP, CropSyst and MACRO comparison in two contrasting soils cropped with maize in Northern Italy, Agr. Water Manage., 97, 1051–1062, 2010.

Childs, C. W.: Towards understanding soil mineralogy. II. Notes on ferrihydrite, Laboratory Report CM7, Soil Bureau, Lower Hutt, New Zealand, 1985.

Civetta, L., Gallo, G., and Orsi, G.: Sr- and Nd-isotope and trace-element constraints on the chemical evolution of the magmatic system of Ischia (Italy) in the last 55 Ka, J. Volcanol. Geoth. Res., 46, 213–244, 1991.

Coppola, A.: Unimodal and bimodal descriptions of hydraulic properties for aggregated soils, Soil Sci. Soc. Am. J., 64, 1252–1262, 2000.

Cruden, D. M. and Varnes, D. J.: Landslides types and processes, in: Landslides: Investigation and Mitigation, Special Report 247. Transportation Research Board, National Research Council, edited by: Turner, A. K. and Schuster, R. J., National Academy Press, Washington, DC, 36–75, 1996.

De Vita, P., Di Clemente, E., Rolandi, M., and Celico, P.: Engineering geological models of the initial landslides occurred on April 30th 2006, at the Mount di Vezzi (Ischia island, Italy), Italian Journal of Engineering Geology and Environment, 2, 119–141, 2007.

De Vita, S., Sansivero, F., Orsi, G., Marotta, E., and Piochi, M.: Volcanological and structural evolution of the Ischia resurgent caldera (Italy) over the past 10 ka, in: Stratigraphy and Geology in Volcanic Areas, edited by: Groppelli, G. and Viereck, L., Geological Society of America Book Series, Special Paper 464, 193–239, 2010.

Di Nocera, S., Matano, F., Rolandi, G., and Rolandi, R.: Contributo sugli aspetti geologici e vulcanologici di Monte di Vezzi (Isola d'Ischia) per lo studio degli eventi franosi dell'aprile 2006, Italian Journal of Engineerig Geology and Environment, 2, 27–50, 2007.

Di Vito, M. A., Sulpizio, R., Zanchetta, G., and D'Orazio, M.: The late Pleistocene pyroclastic deposits of the Campanian Plain: new insights into the explosive activity of Neapolitan Volcanoes, J. Volcanol. Geoth. Res., 177, 19–48, 2008.

FAO: Guidelines for Soil Profile Description, 3rd edn., Soil Resources Management and Conservation Service, Land and Water Development Division, FAO, Rome, revised, 1990.

Fields, M. and Parrott., K. W.: The nature of allophane in soils. III. Rapid field and laboratory test for allophane, New Zeal. J. Sci., 9, 623–629, 1966.

FitzPatrick, E. A.: Micromorphology of Soils, Chapman and Hall, London, 433 pp., 1984.

FitzPatrick, E. A.: Soil Microscopy and Micromorphology, Wiley, West Sussex, England, 304 pp., 1993.

Glendon, G. W. and Dani, O.: 2.4 Particle-size analysis, in: Methods of soil analysis, edited by: Dane, J. H. and Topp, G. C., Part 4, Physical Methods, 255–293, Madison, Wisconsin, USA, Soil Science Society of America, Inc., 2002.
Guzzetti, F. and Tonelli, G.: Information system on hydrological and geomorphological catastrophes in Italy (SICI): a tool for managing landslide and flood hazards, Nat. Hazards Earth Syst. Sci., 4, 213–232, doi:10.5194/nhess-4-213-2004, 2004.
Guzzetti, F., Cardinali, M., and Reichenbach, P.: The AVI Project: a bibliographical and archive inventory of landslides and floods in Italy, Environ. Manage., 18, 623–633, 1994.
Horgan, G. W.: Mathematical morphology for analysing soil structure from images, Eur. J. Soil Sci., 49, 161–173, 1998.
Hungr, O., Evans, S. G., Bovis, M. J., and Hutchinson, J. N.: A review of the classification of landslides of the flow type, Environ. Eng. Geosci., 7, 221–238, 2001.
ISPRA – SINTAI: Progetto Annali. Banca dati, available at: http://www.acq.isprambiente.it/annalipdf/, (last access: 19 December 2014), 2005.
IUSS Working Group WRB: World Reference Base for Soil Resources 2014, International soil classification system for naming soils and creating legends for soil map, World Soil Resources Reports No. 106., FAO, Rome, 2014
Kak, A. C. and Slaney, M.: Principles of Computerized Tomographic Imaging, IEEE Press, Piscataway, NJ, 1988.
Kutilek, M. and Nielsen, D. R.: Soil Hydrology, Catena Verlag, Geoscience Publication, Cremlingen Destedt, Germany, 370 pp., 1994.
Lantuejoul, C. and Maisonneuve, F.: Geodesic methods in quantitative image analysis, Pattern Recogn., 17, 177–187, 1984.
Lesch, S. M. and Suarez, D. L.: A short note on calculating the adjusted SAR index, T. ASABE, 52, 493–496, 2009.
Mazzarella, A. and De Luise, E.: The meteoric event of 30th April 2006 at Ischia island, Italy, Italian Journal of Engineering Geology and Environment, 2, 7–14, 2007.
Mehlich., A.: Use of triethanolamine acetate-barium hydroxide buffer for the determination of some base exchange properties and lime requirement of soil, Soil Sci. Soc. Am. Pro., 29, 374–378, 1938.
Mehra, O. P. and Jackson, M. L.: Iron oxide removal from soils and clays by a dithionite-citrate system buffered with sodium bicarbonate, Clay. Clay Miner., 7, 317–327, 1960.

Orsi, G., de Vita, S., and Di Vito, M.: The restless, resurgent Campi Flegrei nested caldera (Italy): constraints on its evolution and configuration, J. Volcanol. Geoth. Res., 74, 179–214, 1996.
Parfitt, R. L.: Allophane in New Zealand – a review, Aust. J. Soil Res., 28, 343–360, 1990.
Parfitt, R. L. and Wilson, A. D.: Estimation of allophane and halloysite in three sequences of volcanic soils, New Zealand, in: Volcanic Soils: Weathering and Landscape Relationships of Soils on Tephra and Basalt, Catena Suppl. 7, Catena Verlag, Cremlingen, Germany, 1–8, 1985.
Reynolds, W. D. and Elrick, D. E.: The soil solution phase. Falling head soil core (tank) method, in: Methods of Soil Analysis, edited by: Dane, J. H. and Topp, G. C., SSSA Book Ser., vol. 5., SSSA, Madison, WI, USA, 809–812, 2003.
Rittmann, A. and Gottini, V.: L'Isola d'Ischia – geologia, Boll. Serv. Geol. Ital., 101, 131–274, 1980.
Schwertmann, U.: Differenzierung der Eisenoxide des Bodens durch photochemische Extraktion mit saurer Ammoniumoxalat-losung, Lösung. Z. Pflanzenernäh. Düng. Bodenk., 105, 194–202, 1964.
Serra, J.: Image Analysis and Mathematical Morphology, Academic Press, London, 1982.
Shoji, S., Dahlgren, R., and Nanzyo, M.: Genesis of volcanic ash soils, in: Volcanic Ash Soils. Genesis, Properties and Utilization. Developments in Soil Science, 21, Elsevier, Amsterdam, London, New York, Tokyo, 37–71, 1993.
Terribile, F., Basile, A., De Mascellis, R., Di Gennaro, A., Mele, G., and Vingiani, S.: I suoli delle aree di crisi di Quindici e Sarno: proprietà e comportamenti in relazione ai fenomeni franosi, Quaderni di Geologia Applicata, 7, 59–79, 2000.
Terribile, F., Basile, A., De Mascellis, R., Iamarino, M., Magliulo, P., Pepe, S., and Vingiani, S.: Landslide processes and andosols: the case study of the Campania region, Italy, in: Soils of Volcanic Regions in Europe: Volcanic Soils and Land Use, edited by: Arnalds, Ó., Bartoli, F., Buurman, P., Óskarsson, H., Stoops, G., García-Rodeja, E., Springer, Berlin, Heidelberg, New York, 545–563, 2007.
Vezzoli, L.: Island of Ischia, C.N.R. Quaderni de la "Ricerca Scientifica", P.F.G., 114, 51–72, 1988.
Vingiani, S. and Terribile, F.: Soils of the detachment crowns of Ischia landslides, Italian Journal of Engineering Geology and Environment, 2, 51–63, 2007.

Walkley, A. and Black, I. A.: An examination of the Degtjareff method for determining organic carbon in soils: effect of variations in digestion conditions and of inorganic soil constituents, Soil Sci., 63, 251–263, 1934.
Ward, S. and Day, S.: The 1963 landslide and flood at Vaiont Reservoir Italy. A tsunami ball simulation, Boll. Soc. Geol. Ital., 130, 16–26, 2011.
Watson, K. K.: An instantaneous profile method for determining the hydraulic conductivity of unsaturated porous materials, Water Resour. Res., 2, 709–715, 1966.
Wells, N. and Furkert, R. J.: Bonding of water to allophane, Soil Sci., 113, 110–115, 1972.

Table 1. Field morphology description of the studied soil profiles.

Profile	Horizon	Depth (cm)	Moistness	Colour (moist)	Structure	Roots	Rock fragments
P1	A	0–5	sm	10YR 3/2	we to mo fi GR	vf F	f A
	Bw1	5–18	sm	10YR 4/4	we to mo me SB	f V	m A
	Bw2	18–55	m	2.5Y 4/3	we to mo SB	vf F	m M
	2BC	55–70	sm	2.5Y 4/3	we SB me to MA	N	m M
	2C	70/90–110/120	sm	2.5Y 5/2	MA	N	f V
	2Btb	110/120–170+	sm	10YR 4/4	mo me SB	N	f V
P2	A	0–5	sm	10YR 2/2	we fi GR	vf F	f F
	Bw1	5–50	sm	10YR 4/4	we me SB	f V	f C
	Bw2	50–90/110	sm	10YR 4/4	we co SB	f F	m A
	Bw3	110–130/140	sm	2.5Y 4/4	we co SB	c V	fm A
	Bw4	140–170	sm	2.5 Y 4/3	we me SB	f V	m M
	2CB	170–180/205	sm	2.5 Y 4/3	we SB me to MA	f V	f V
	2C	205–215+	sm	2.5 Y 5/2	MA	N	N
P3	A	0–5	sm	10YR 2/2	mo fi GR	vf F	m F
	Bw1	15–50	sm	10YR 4/4	we me SB	f F	fm C
	Bw2	50–85	sm	10YR 4/4	we co SB	vf V	c A
	Bw3	85–135	sm	2.5 Y 4/3	we me SB	vf V	m M
	Bw4	135–190	sm	2.5 Y 4/3	we me SB	vf F	m M
	2C	190–220	sm	2.5 Y 6/2	we SB me to MA	N	N
	2Bt	220–260+	sm	10YR 5/4	mo me SB	N	N

Legend (according to FAO, 2006):
Soil structure;
grades: we = weak; mo = moderate; st = strong;
size classes: co = coarse; vc = very coarse; me = medium; fi = fine;
types: GR = granular; CR = crumbly; AB= angular blocky; PR = prismatic; SB = subangular blocky; MA = massive; SG = single grain;
Moistness;
sm = slightly moist, m = moist, w = wet;
Roots;
diameter: vf = very fine, f = fine, m = medium, c = coarse;
abundance: N = none, V = very few, F = few, C = common, M = many;
Rock fragments;
size classes: f = fine, m = medium, c = coarse, s = stones, b = boulders, l = large boulders;
abundance: N = none, V = very few, F = few, C = common, M = many, A = abundant, D = dominant, S = stone line.

Table 2. Soil chemical properties.

Profile	Horizon	OC	pH			Δ pH	CEC	Na	Ca	Mg	K	BS	ESP	EC	SAR
		$g\,kg^{-1}$	H_2O	KCl	NaF		$cmol^{(+)}\,kg^{-1}$	%	%	%	%	%	%	$\mu S\,cm^{-1}$	
P1	A	46.1	6.9	5.8	9.5	1.1	20.7	6	64	21	9	100	5.8	n.d.	0.4
	Bw1	12.3	6.8	5.4	10.3	1.4	15.1	12	38	24	25	66	7.9	n.d.	0.7
	Bw2	4.1	7.0	4.9	9.4	2.1	13.5	10	19	47	23	100	10.4	n.d.	0.7
	2BC	3.1	7.4	5.2	9.2	2.2	14.0	17	34	23	26	100	17.1	75.8	1.2
	2C	0.8	7.6	5.1	8.8	2.5	10.5	23	30	25	22	100	22.9	50.7	1.4
	2Btb	0.9	7.4	5.0	9.0	2.4	15.6	24	32	27	17	100	63.0	102.2	1.4
P2	A	71.3	6.7	6.0	9.5	0.7	36.8	3	73	19	4	100	3.3	n.d.	0.3
	Bw1	5.9	7.1	5.7	9.9	1.4	10.7	10	46	23	21	94	9.3	n.d.	0.5
	Bw2	5.6	7.4	5.9	10.1	1.5	9.4	13	48	20	19	90	11.7	n.d.	0.6
	Bw3	4.7	7.1	5.1	10.0	2.0	13.0	15	46	15	25	90	13.1	n.d.	0.9
	Bw4	2.7	7.3	5.4	9.7	1.9	10.8	18	44	13	25	100	17.6	73.6	1.1
	2CB	1.3	7.2	5.0	9.5	2.2	12.4	19	35	23	23	100	18.5	59.6	1.2
	2C	1.2	7.3	4.8	9.0	2.5	9.9	35	4	30	30	90	31.3	64.8	2.5
P3	A	49.4	6.7	6.0	9.6	0.7	28.6	5	63	22	11	100	4.5	n.d.	0.4
	Bw1	6.0	6.0	4.2	9.9	1.8	16.2	13	43	24	21	80	10.5	n.d.	0.8
	Bw2	2.9	6.9	5.0	9.7	1.9	15.1	13	45	23	20	94	11.9	n.d.	0.8
	Bw3	3.6	7.1	5.2	9.7	1.9	10.7	13	39	26	21	96	13.1	n.d.	0.8
	Bw4	2.3	7.2	5.2	9.4	2.0	8.5	18	34	28	20	100	17.6	58.7	0.9
	2C	1.2	7.2	5.2	9.5	2.0	11.6	17	30	36	17	100	17.2	63.3	1.0
	2Btb	1.1	7.1	5.2	9.2	1.9	15.2	19	36	28	18	100	19.1	127.1	1.3

BS = base saturation calculated as $\sum$bases · 100/CEC;
ESP = Exchangeable Sodium Percentage;
SAR = sodium adsorption ratio;
ΔpH = calculated as difference between pH H_2O and pH KCl.

Table 3. Particle size distribution (PSD) and saturated hydraulic conductivity (k_s).

Profile	Horizon	sand	silt	clay	* coarse fragments	Textural classes	k_s	
		%	%	%	%		$cm\,h^{-1}$	$cm\,s^{-1}$
P1	A	57.8	39.0	3.2	16.0	SL		
	Bw1	49.0	45.4	5.7	13.4	SL		
	Bw2	49.3	44.8	5.9	6.2	SL		
	2BC	35.5	55.8	8.6	20.3	SiL		
	2C	36.5	56.6	6.9	0.9	SiL		
	2Btb	n.d.	n.d.	n.d.	n.d.			
P2	A	57.7	39.9	2.4	3.1	SL		
	Bw1	53.8	40.9	5.2	11.1	SL	1.03E+02	2.86E−02
	Bw2	55.3	39.7	5.0	25.5	SL	1.35E+02	3.75E−02
	Bw3	43.9	50.2	5.9	8.9	SL		
	Bw4	36.1	54.5	9.4	4.2	SiL	8.07E+01	2.24E−02
	2CB	28.4	63.9	7.7	1.0	SiL	2.33E+01	6.47E−03
	2C	24.6	68.8	6.6	0.1	SiL	5.50E+00	1.53E−03
P3	A	50.7	45.8	3.5	8.0	SL		
	Bw1	51.0	43.1	5.9	20.9	SL		
	Bw2	46.7	47.3	6.1	10.5	SL		
	Bw3	41.3	50.6	8.1	11.1	SiL		
	Bw4	48.5	44.7	6.9	8.0	SL	2.00E+02	5.56E−02
	2C	33.1	59.2	7.7	1.3	SiL	1.06E+01	2.94E−03
	2Btb	38.9	55.2	5.9	0.7	SiL	2.40E+01	6.67E−03

* rock fragments = percentage of the total bulk soil;
n.d = not determined.

Table 4. Selectively dissolved elements (Al, Fe, Si) measured by ICP-AES.

Profile	Horizon	Al_o	Fe_o	Si_o	Al_p	Fe_d	$Al_o + 0.5Fe_o$	Pret	Al_p/Al_o	Fe_o/Fe_d	Allophane	Ferrihydrite
		$g\,kg^{-1}$	$g\,kg^{-1}$	$g\,kg^{-1}$	$g\,kg^{-1}$	$g\,kg^{-1}$	%	%			%	%
P1	A	2.8	2.3	3.1	0.4	3.8	0.4	25	0.2	0.61	1.6	0.4
	Bw1	5.2	3.5	4.9	0.5	5.0	0.7	34	0.1	0.69	2.6	0.6
	Bw2	2.0	1.8	2.7	0.1	4.6	0.3	19	0.1	0.38	1.4	0.3
	2BC	1.7	1.2	2.6	0.1	4.5	0.2	16	0.0	0.27	1.3	0.2
	2C	0.5	0.3	1.9	0.1	1.9	0.1	2	0.3	0.17	0.8	0.1
	2Bwb	n.d.	n.d.	n.d.	n.d.	n.d.	n.d.	n.d.	n.d.	n.d.	n.d.	n.d.
P2	A	3.5	2.5	3.6	0.7	3.9	0.5	32	0.2	0.65	1.8	0.4
	Bw1	3.3	2.0	4.6	0.1	3.5	0.4	22	0.0	0.58	2.3	0.3
	Bw2	3.9	1.8	5.0	0.1	3.3	0.5	20	0.0	0.54	2.6	0.3
	Bw3	1.8	1.5	2.5	0.1	3.8	0.3	17	0.0	0.40	1.3	0.3
	Bw4	1.6	1.0	2.4	0.0	3.7	0.2	15	0.0	0.27	1.2	0.2
	2CB	0.8	0.4	2.2	0.2	2.6	0.1	8	0.2	0.17	1.0	0.1
	2C	0.5	0.3	2.0	0.2	2.2	0.1	4	0.4	0.15	0.9	0.1
P3	A	3.1	2.0	3.4	0.3	4.3	0.4	27	0.1	0.47	1.8	0.3
	Bw1	2.2	1.2	2.8	0.1	4.3	0.3	21	0.1	0.27	1.4	0.2
	Bw2	2.2	1.0	3.0	0.0	4.1	0.3	18	0.0	0.23	1.5	0.2
	Bw3	1.3	0.8	2.5	0.1	3.6	0.2	12	0.0	0.23	1.2	0.1
	Bw4	0.7	0.5	2.1	0.1	2.5	0.1	8	0.1	0.19	1.0	0.1
	2C	0.6	0.4	2.2	0.1	2.2	0.1	5	0.1	0.18	1.0	0.1
	2Btb	0.8	0.4	2.2	0.3	3.1	0.1	9	0.3	0.13	1.0	0.1

Al_o, Fe_o, Si_o = ammonium oxalate extractable aluminium, iron and silicium;
Al_p = Na-pyrophosphate extractable aluminium; Fe_d = Na-dithinite citrate-bicarbonate extractable iron; Pret = phosphate retention; Allophane = calculated following the Parfitt and Wilson (1985) formula = $100 \cdot \%Si_o / \{-5.1 \cdot [(Al_o - Al_p)/Si_o] + 23.4\}$;
Ferrihydrite = calculated following the Childs formula = $\%Fe_o \cdot 1.7$.

Table 5. Comparison between data of porosity obtained by hydrological and microtomographic measurements

	Porosity %		
Soil horizons	Hydrological data	Inter-aggregate by microtomography*	pores between 30 and 1.5 µm
Bw4	61	36	25
2CB	57	15	42
2C	61	7	54

* more than 30 µm resolution.

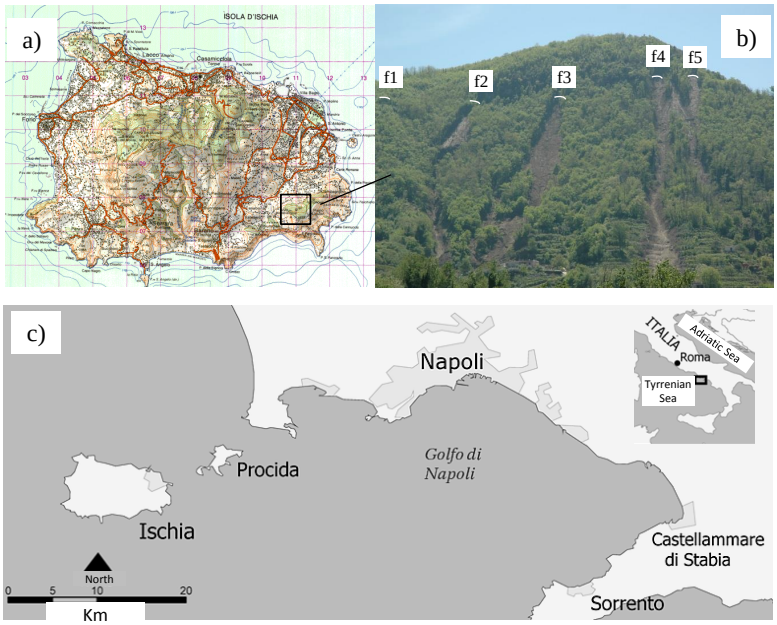

Figure 1. (a) Topographic map in scale 1 : 50 000 of Ischia, **(b)** the Northern slope of Mt. Vezzi, in which both positions and names (by Ascione et al., 2007) of the 5 detachment crowns have been reported, **(c)** location of the Ischia island ahead the Golfo di Napoli (southern Italy).

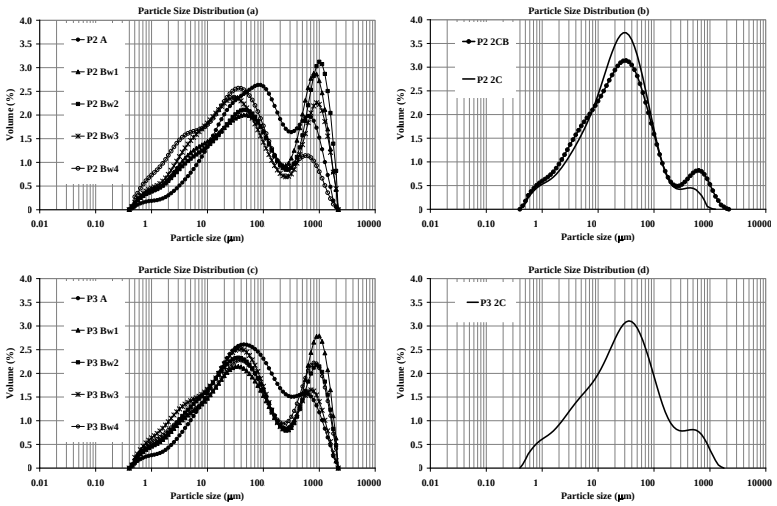

Figure 2. Particle size distribution (PSD) of: **(a)** A and Bw horizons of P2 and **(b)** 2CB and 2C horizons of P2; **(c)** A and Bw horizons of P3 and **(d)** 2C horizon of P3.

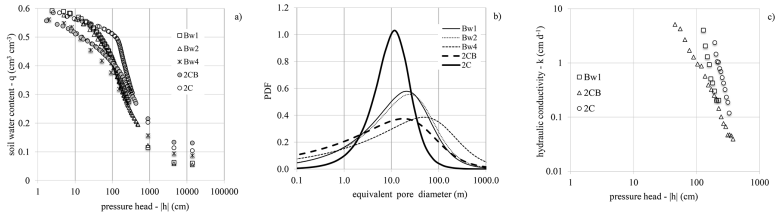

Figure 3. Hydraulic properties of selected horizons of the P2: **(a)** water retention curves, **(b)** equivalent pore size distributions and **(c)** hydraulic conductivity curves.

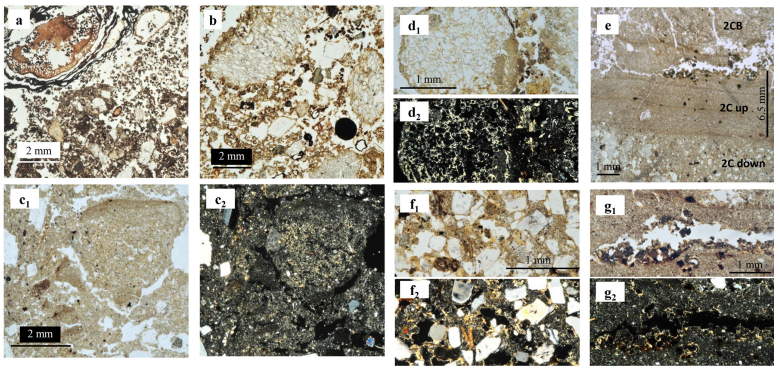

Figure 4. Optical microscopy: **(a)** very fine granular structure, presence of living roots and decomposed organic residues in the A horizon; **(b)** granular structure, showing very abundant (from 25 to 50 %) poorly weathered pumice fragments, enveloped by silty – fine sandy brown material, in the Bw horizon; **(c)** angular to sub-angular aggregates, pseudo-stratified by finer brownish and coarser materials, which are chaotically immersed in the soil matrix of the 2CB horizon (c1 and c2 in PPL and XPL, respectively); **(d)** weathering and neogenetic clays in a pumice and clay coating fragments in a root pore (d1 and d2 in PPL and XPL, respectively); **(e)** transition from 2CB towards the finely stratified upper part of 2C; **(f)** lower coarser part of 2C, having a mineral granular structure with pores empty by clay infillings (f1 and f2 in PPL and XPL, respectively); **(g)** root pore at the boundary 2CB–2C, in which anisotropic clay films and frequent Fe-Mn segregations coat the walls (g1 and g2 in PPL and XPL, respectively).

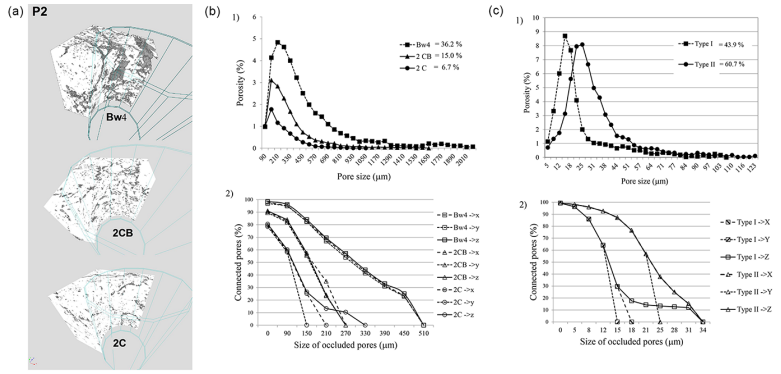

Figure 5. Microtomographic analysis: **(a)** 1.5 cm × 1.5 cm × 1.5 cm ROIs (regions of interests) of 3 soil horizons from P2 profile reconstructed by X-ray MicroCT (30 µm image resolution); **(b)** inter-aggregate (1) Pore Size Distribution (PoSD) and (2) percolation Curves (Pore Connectivity) by 3-D image analysis of Bw4, 2CB and 2C of P2. The intersections between the percolation curves and the abscissa represent the percolation threshold (pt) of the samples; **(c)** intra-aggregate (1) PoSD and (2) Pore Connectivity by 3-D image analysis of the two selected aggregates (Type I and Type II) from 2C of P2.

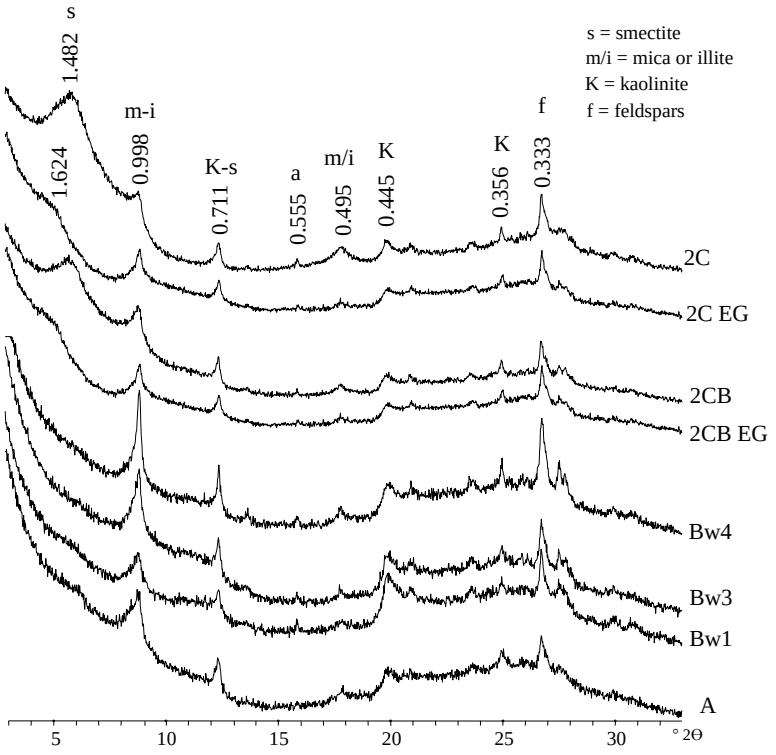

Figure 6. XRD patterns of untreated and treated (EG = ethylene glycol solvated) clay samples separated by soil horizons of the P2 profile.